Investigation of an extreme rainfall event during 8–12 December 2018 over central Viet Nam – Part 2: An evaluation of predictability using a time-lagged cloud-resolving ensemble system

Chung-Chieh Wang[1], Duc Van Nguyen[1,2], Thang Van Vu[2], Pham Thi Thanh Nga[2], Pi-Yu Chuang[1], and Kien Ba Truong[2,*]

Correspondence: kien.cbg@gmail.com

[1]Department of Earth Sciences, National Taiwan Normal University, Taipei, Taiwan

[2]Viet Nam Institute of Meteorology, Hydrology and Climate Change, Hanoi, Viet Nam

Abstract:

This is the second part of a two-part study that investigates an extreme rainfall event that occurred from 8 to 12 December 2018 over central Viet Nam (referred to as the D18 event). In this part, the study aims to evaluate the predictability of the D18 event using a time-lagged cloud-resolving ensemble and a quantitative precipitation forecast system. To do this study, 29 time-lagged (8 days in lead time) high resolution (2.5 km) members were run, with the first members run at 12:00 UTC 3 December 2018, and the last member-run at 12:00 UTC 10 December 2018. Between the first and the last members are multiple members that run every 6-h. The evaluated results reveal that the could-resolving model (CReSS) well predict the rainfall fields at the short-range forecast (less than 3 days) for 10 December (rainiest day). Particularly, results show CReSS has high skills in heavy-rainfall quantitative precipitation forecasts (QPFs) for the 24-h rainfall of 10 Dec with the Similarity Skill Score (SSS) scores greater than 0.5 for both the last five members and the last nine members. These good results are due to the model having good predictionspredicts of other meteorological variables, such as surface wind fields. However, these prediction skills are reducing at extending lead time (longer than 3 days), and it is challenging to achieve the prediction of QPF for rainfall thresholds greater than 100 mm with lead time longer than 6 days. Besides, the ensemble sensitivity analysis of 24-hour rainfall responds to the initial conditions shows that the 24-hour rainfall is very sensitive with initial

conditions, not only at the lower level but also at the upper level. The ensemble-based sensitivity is decreased with the increasing lead time. Through the analysis of thermodynamic and moisture sensitivities, it showed that the features of the ensemble-based sensitivity analysis (ESA) facilitated a better understanding of the sensitivity of a precipitation forecast to the initial conditions, implying that it is meaningful to apply ESA to control initial conditions by work in the future.

1 Introduction

The present study is the second part of a two-part study investigating the extreme rainfall event during 8–12 December 2018 over central Viet Nam (referred to as the D18 event hereafter). D18 event is a record-breaking rainfall event which occurred along the mid-central coast, from Quang Binh to Quang Ngai provinces. The observational data shows that particularly heavy rainfall with the maximum 3-days accumulated rainfall from 12:00 UTC on 8 December to 12:00 UTC on 11 December exceeding 800 mm (Fig. 1f). In which, the rainiest day is 10 December with 24-h observed data exceed 600 mm at some stations (Fig. 4 OBS). This record-breaking rainfall event led to 13 dead, many destructions in the environment, downstream cities, and many other economic losses due to catastrophic flooding and landslides (Tuoi Tre news, 2018). In part 1 (Wang and Nguyen 2023), we focused on the analysis of the mechanism that caused this event and evaluated the simulation by the Cloud-Resolving Storm Simulator (CReSS; Tsuboki and Sakakibara, 2002, 2007). The analyzed results point out the main factors which led to this event as well as its spatial rainfall distribution. These factors included the combined interaction between the strong northeasterly winds and easterly winds over the South China Sea (SCS) in the lower troposphere (below 700 hPa). The local terrain also played essential role due to its barrier effect. The cloud model's good simulation results in part 1 indicated its promising potential in forecasting this event. Hence, in part 2, the present study focuses on an evaluation of its predictability of the D18 event through a series of time-lagged high resolution ensemble quantitative precipitation forecasts (QPFs) by the CReSS model.

55 Until now, predicting heavy rainfall events is still challenging to meteorologists and
56 weather forecasters, although great progresses in both computer science and atmospheric
57 science have been made to improve predictability. The prediction of heavy to extreme
58 rainfall is more difficult for Viet Nam, where both multi-scale interactions among different
59 weather systems and strong influence by local topography often exist. For example, when
60 D18 event occurred, several operational models were unable to predict this event
61 successfully. Specifically, Fig. 1 shows the predictions for the D18 event by three global
62 models at the National Centers for Environmental Prediction (NCEP), the European Centre
63 for Medium-Range Weather Forecasts (ECMWF), and the Japan Meteorological Agency
64 (JMA), and by one mesoscale regional model, the Weather Research and Forecasting
65 (WRF) model, implemented for operation at the Mid-central regional Hydro-
66 Meteorological center in Da Nang city, Viet Nam. While these models overall made good
67 predictions in the surface wind field, their 72-h accumulated rainfall amounts along the
68 coast of central Viet Nam (less than 250 mm) were much lower than the observation, which
69 exceeded 900 mm (Fig. 1). Therefore, in order to improve the QPFs for heavy rainfall
70 events in Viet Nam, we need to not only understand their mechanisms of occurrence, but
71 also develop better forecasting tools.

72
73
74
75
76

77
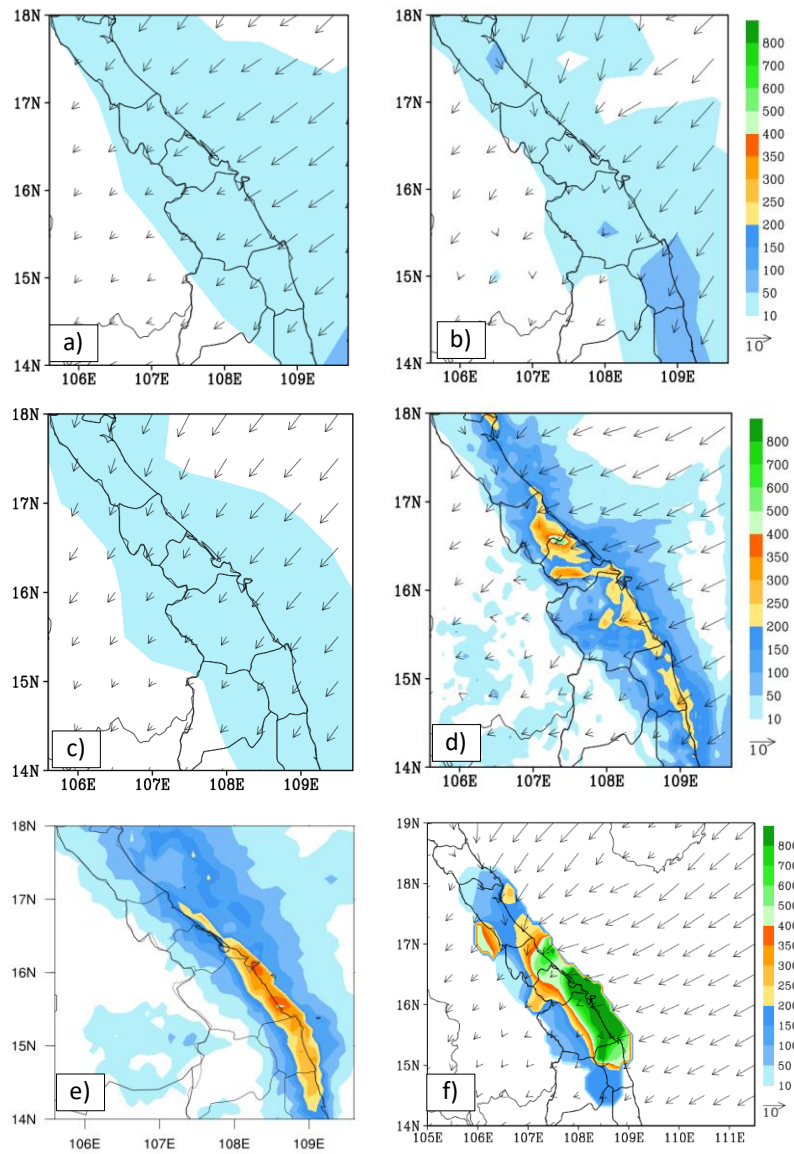
Figure 1. The predicted 72h accumulated rainfall (mm, shaded) and mean surface wind
(ms^{-1}, vector) for the period of 12:00 UTC 8 December – 12:00 UTC 11 December 2018

obtained by (a) NCEP, (b) ECMWF, (c) JMA, (d) WRF, (e) 72h accumulated rainfall obtained by the Global Precipitation Measurement (GPM) estimate (IMERG Final Run product) and (f) 72h in-situ observed accumulated rainfall (mm, shaded) and the mean surface wind derived from ERA5 data (ms^{-1}, vector), adapted from Fig. 14c of Wang and Nguyen 2023.

Among several different methods, the present-day weather forecasts depend mainly on numerical weather prediction (NWP) using models, a scientific method that has become indispensable for its ability to simulate weather and produce quantitative results (Fig. 1). However, there is always uncertainty in the numerical forecasts due to the fact that the atmosphere is a chaotic system and tiny errors in the initial state can grow rapidly and lead to large errors in the forecast (Hohenegger and Schär, 2007, Lorenz 1969). Various approximations in numerical methods are also sources of forecast uncertainty. Thus, by generating a range of possible weather conditions in days ahead or into the future, the ensemble forecasting was introduced as an effective method to estimate forecast uncertainty and improve the overall accuracy and usefulness of NWP products. For example, some studies have shown high skill in QPFs for extreme rainfall produced by typhoons in Taiwan using the CReSS model, a cloud-resolving model (CRM), with high resolution and time-lagged approach (Wang et al. 2016; Wang 2015; Wang et al. 2014; Wang et al. 2013). Table 1 of Wang et al. (2016) shows that the high-resolution time-lagged ensemble forecasts provide overall better quality in comparison with both the traditional low-resolution ensemble forecasts and high-resolution deterministic forecasts at a comparable cost in computation. Furthermore, some studies show that the ensemble mean typically has smaller errors than individual members (Murphy 1988, Surcel et al. 2014). This error reduction is because the high predictability features that the members agree on are emphasized by the mean, while the low-predictability ones that the members do not agree on are filtered out or dampened (e.g., Leith 1974; Murphy 1988, Surcel et al. 2014).

Besides the advantages of ensemble forecasts described above, the ensemble-based sensitivity analysis ~~(ESA)~~ also helps effectively investigate how sensitive the forecast variables are and to what preceding factors. To be more specific, Torn and Hakim (2009) used ESA to evaluate how their subject, tropical cyclones (TCs) undergoing extratropical transition, in the prediction respond to a change in the initial condition. In their results, the cyclone minimum sea-level pressure forecasts are determined as strongly sensitive to TC intensity and position at short lead times and equally sensitive to mid-latitude troughs that interacted with the TC at longer lead times. For an extreme rainfall event in northern Taiwan, Wang et al. (2021) performed ESA using the results from 45 forecast members with a grid size of 2.5–5 km to identify contributing factors to heavy rainfall. By normalizing their impacts on rainfall using standard deviation (SD), different factors can be compared quantitatively and on an equal footing. Ranked by their importance, these factors included the position of the surface Mei-yu front and its moving speed ~~(−16.00 mm per 5 km h⁻¹)~~, the position of 700-hPa wind shift line and its speed ~~(+12.59 mm per 0.4° latitude)~~, the moisture amount in the environment near the front ~~(+11.73 mm per 0.92 g kg⁻¹ in mixing ratio)~~, timing and location of frontal mesoscale low-pressure disturbance ~~(+11.03 mm per1.38° longitude)~~, and ~~(5)~~ frontal intensity ~~(+9.58 mm per 3 K in equivalent potential temperature difference across 0.5°)~~. Many other studies also used the ESA to study TCs, convective events, or support the development of operational ensemble sensitivity-based techniques to improve probabilistic forecasts (Kerr et al. 2019, Hu and Wu 2020, Coleman and Ancell 2020).

For heavy precipitation over central Viet Nam, Son and Tan (2009) used the Mesoscale Model version 5 (MM5) to investigate the predictability of heavy rainfall events over the southern part of central Viet Nam during the period of 2005 and 2007. In this study, experiments were configured for two domains with the horizontal resolutions of the mother domain and the nest domain are 27km and 9km, respectively. Their results showed that MM5 can predict heavy rainfall there and its performance is better for events caused by TCs or TC interactions with the cold air. Toan et al. (2018) assessed the predictability of

heavy rainfall events in middle-central Viet Nam due to combined effects of cold air and easterly winds using the WRF model within a forecast range of 2 days. The model was set with two domains using the nesting technique. The outermost domain (D1) covers entirely Vietnam and South China Sea with horizonal resolution of 18 km, while the inner domain (D2) focuses on the Mid-Central Vietnam region with horizonal resolutions of 6km. The evaluation indicated that for 24-h lead time, the model performed reasonably well at rainfall thresholds less than 100 mm day^{-1}. For 48-h forecast range, the model performed well only at thresholds below 50 mm day^{-1} and had some skill at 50–100 mm day^{-1}. However, heavy rainfall events at thresholds over 100 mm day^{-1} were almost unpredictable by the model. Nhu et al. (2017) also used the WRF model to investigate the role of the topography in central Viet Nam on the occurrence of a heavy rainfall event there in November 1999. In this study, the model with 3 nested domains with horizontal resolution of 45km, 15km, 5km and 47 vertical levels well simulated the northeast monsoon circulation, TCs, and the occurrence of heavy rainfall in central Viet Nam. Furthermore, when the topography is removed, the three-day total accumulated rainfall decreased sharply (by approximately 75%) compared to that in the control experiment with the terrain. Hoa Van Vo (2016) examined the predictability of heavy-rainfall events during the wet seasons of 2008−2012 in the middle section and central highlands of Viet Nam using NWP products from several global models, including the Global Forecasting System (GFS) from NCEP, Global Spectral Model (GSM) from JMA, Navy Operational Global Atmospheric Processing System (NOGAPS) from the US Navy, and the Integrated Forecast System (IFS) from ECMWF. Their results indicated that IFS and GSM performed better than GFS and NOGAPS, and IFS was evaluated the best. However, all four global models under-estimated rainfall in extreme events. One of the reasons for this under-estimated rainfall is that these models are global models, so their resolutions are coarse while the study area is too small.

The review above suggests that considerable limitations still exist in forecasting heavy rainfall in central Viet Nam, especially using coarser models. It also indicates that a high-

163 resolution time-lagged ensemble approach may offer some advantages in the prediction of
164 extreme rainfall events, such as a better simulation of local weather conditions, a quicker
165 response to changes in forecast uncertainty in real time, and potentially a longer lead time
166 for hazard preparation. Climatologically, the entire Viet Nam lies in the tropical zone (Fig.
167 2a), where vigorous but less organized convection often develops in response to local
168 conditions, while the region is also prone to the influence and interactions of weather
169 systems spanning a wide range of scales as reviewed. In addition, although central Viet
170 Nam is a small region with the narrowest place only about 80 km in width, it possesses
171 significant topography running in the north-south direction to affect rainfall (Fig. 2a).
172 Hence, a high-resolution CRM with detailed and explicit treatment in cloud microphysics
173 is likely crucial for better QPFs in central Viet Nam. Consequently, the present study used
174 the CReSS model to investigate the predictability of the D18 event through a series of time-
175 lagged ensemble predictions. The rest of this paper is organized as follows. Section 2
176 describes the data, model, and methodology used in the study. The model results are
177 presented and evaluated in Section 3. Finally, conclusions are offered in Section 4.

178 **2 Data and methodology**

179 2.1 Data

180 2.1.1 Model validation

181 *2.1.1.1 In-situ observation data*

182 The daily in-situ observed rainfall data (12:00–12:00 UTC, i.e., 19:00–19:00 LST) from 8
183 to 12 December 2018 at 69 automated gauge stations across central Viet Nam is used for
184 case overview and verification of model results. This dataset is provided by the Mid-
185 Central Regional Hydro Meteorological Center, Viet Nam. The spatial distribution of these
186 gauge stations is depicted in figure 2b.

187 *2.1.1.2 The Global Precipitation Measurement (IMERG Final Run V07) data*

The Global Precipitation Measurement (GPM) is a mission international jointly by the National Aeronautics and Space Administration (NASA) and the Japan Aerospace Exploration Agency (JAXA), employing an international satellite network for advanced global rain and snow observations. The GPM *IMERG Final Run* is a research-level product which is created by intercalibrate, merging, and interpolating "all" satellite microwave precipitation estimates, along with microwave-calibrated infrared (IR) satellite estimates, analyses from precipitation gauges, and potentially other precipitation estimation methodologies at fine time and space scales. The horizontal resolution of this dataset is 0.1º ×0.1º latitude–longitude and the time resolution is every 30 minute (). In this study, we used this satellite data (version 7) to verify rainfall distribution over the coastal sea due to the limitation of the observation station network, we only have the observation stations inland, as shown in the Fig. 2b. This dataset was downloaded from 12:00 UTC on 8 December to 12:00 UTC on 11 December 2018 to analyze the D18 event as well as the rainiest day of this event (10 December).

2.1.1.3 NCEP GDAS/FNL global tropospheric analyses data

The present study used this data (version d083003) to verify the initial data and the model output. The NCEP FNL analysis data is an operational global gridded analysis data and is freely provided by NCEP. The horizontal resolution of this dataset is 0.25º × 0.25º latitude–longitude with 26 levels extending from the surface to 10 hPa. The temporal resolution is 6 hours. Variables have been used in this study including the zonal and meridional wind components, relative humidity and vertical velocity at 925 hPa, and downloaded from 18:00 UTC 04 to 12:00 UTC 09 December 2018.

2.1.2 The added values of CReSS ensemble

2.1.2.1 The International Grand Global Ensemble retrieval

In this study, we used the global model predictions to analyze the predictability of the D18 event. The International Grand Global Ensemble (TIGGE) retrieval is a key component of The Observing System Research and Predictability Experiment (THORPEX) research

program, whose aim is to accelerate the improvements in the accuracy of 1-day to 2-week high-impact weather forecasts. The TIGGE retrieval provides not only deterministic forecast data but also ensemble prediction datasets from major centers, including NCEP of the USA, ~~MetOffice of the United Kingdom (UKMO)~~, ECMWF of the European countries~~European Union~~, and JMA of Japan, since 2006. This dataset has been used for a wide range of research studies on predictability and dynamical processes. ~~In this study, we used the global model predictions to analyze the predictability of the D18 event.~~ In this study, ~~T~~the variables utilized included total precipitation and surface winds (*u*- and *v*-wind components at 10-m height) from NCEP, ECMWF, and JMA at 6-h intervals during our data period (as shown in Figs. 1a-c) from 12:00 UTC 8 to 12:00 UTC 11 December 2018 (as shown in Figs. 1a-c). The data linked is placed in the "code and data availability" section.

~~2.1.2 NCEP GFS historical archive~~

~~In this study, the NCEP GFS data from the analyses and forecast runs executed every 6 h, at 00:00, 06:00, 12:00, and 18:00 UTC daily, were used to drive the CReSS model predictions. The horizontal resolution of the data is 0.25° × 0.25°, and 26 of vertical levels, and the forecast fields are provided every 3 h from the initial time out to a range of 192 h. The data linked is also placed in the "code and data availability" section.~~

~~2.1.3 Observation data~~

~~The daily observed rainfall data (12:00–12:00 UTC, i.e., 19:00–19:00 LST) from 8 to 12 December 2018 at 69 automated gauge stations across central Viet Nam is used for case overview and verification of model results. This dataset is provided by the Mid Central Regional Hydro Meteorological Center, Viet Nam. The spatial distribution of these gauge stations is depicted in figure 2b.~~

~~2.1.4 The Global Precipitation Measurement (IMERG Final Run) data~~

~~The Global Precipitation Measurement (GPM) is a mission international jointly by the National Aeronautics and Space Administration (NASA) and the Japan Aerospace~~

242 ~~Exploration Agency (JAXA), employing an international satellite network for advanced~~
243 ~~global rain and snow observations. The GPM *IMERG Final Run* is a research-level product~~
244 ~~which is created by intercalibrate, merging, and interpolating "all" satellite microwave~~
245 ~~precipitation estimates, along with microwave-calibrated infrared (IR) satellite estimates,~~
246 ~~analyses from precipitation gauges, and potentially other precipitation estimation~~
247 ~~methodologies at fine time and space scales. The horizontal resolution of this dataset is 0.1º~~
248 ~~×0.1º latitude-longitude and the time resolution is every 30 minute. In this study, we used~~
249 ~~this satellite data to verify rainfall distribution over the coastal sea due to the limitation of~~
250 ~~the observation station network, we only have the observation stations inland, as shown in~~
251 ~~the Fig. 2b. This dataset was downloaded from 12:00 UTC on 8 December to 12:00 UTC~~
252 ~~on 11 December 2018 to analyze the D18 event as well as the rainiest day of this event (10~~
253 ~~December).~~

254 *2.1.2.52 The WRF data*

255 The WRF is implemented for operational numerical forecast system at Mid-central regional
256 Hydro- Meteorological center, Viet Nam. In this study, we used this data to analysis the
257 predictability of D18 event using the mesoscale numerical prediction. The download
258 variables include precipitation, the surface U wind component and surface V wind
259 component. The lead time is 3 days, starting from 12:00 UTC 8 to 12:00 UTC 11 December
260 2018 with interval time of 6 hours. The horizontal resolution of this data is 6 km x 6 km.

261 2.2 Model description and experiment setup

262 We used the could-resolving model (CReSS). This model had been built and developed by
263 Nagoya University, Japan (Tsuboki and Sakakibara, 2002, 2007). This is a non-hydrostatic
264 and compressible cloud model, designed for simulation of various weather events at high
265 (cloud-resolving) resolution. In the model, the cloud microphysics is treated explicitly at
266 the user-selected degree of complexity, such as the bulk cold-rain scheme with six species:
267 vapor, cloud water, cloud ice, rain, snow, and graupel (Lin et al., 1983; Cotton et al., 1986;
268 Murakami, 1990, 1994; Ikawa and Saito, 1991). Other subgrid-scale processes

269 parameterized, such as turbulent mixing in the planetary boundary layer, as well as physical

270 options for surface processes, including momentum/energy fluxes, shortwave and

271 longwave radiation are summarized in Table 1.

272 Besides, the NCEP GFS data (version ds084.6) from the analyses and deterministic

273 forecast runs executed every 6 h, at 00:00, 06:00, 12:00, and 18:00 UTC daily, were used

274 to drive the CReSS model predictions. The horizontal resolution of the data is $0.25° \times$

275 $0.25°$, and 26 of vertical levels, and the forecast fields are provided every 3 h from the

276 initial time out to a range of 192 h. The data linked is also placed in the "code and data

277 availability" section.

278

279 To evaluate of the predictability of the D18 event using an ensemble time-lagged high-

280 resolution system and investigate the ensemble sensitivity of variables for the rainfall, 29

281 experiments were performed. The first members was initialized ran at 12:00 UTC on 3

282 December 2018, and the last member was initialisedran at 12:00 UTC on 10 December

283 2018. A new member was initialised every 6-hr within the period 1200 UTC 3 Dec 2018-

284 1200 UTC 10 Dec 2018 Between the first and the last members are multiple members

285 running every 6 h (for a simulation length of 192 h).

286 All experiments using a single domain at 2.5 km horizontal grid spacing and a (x, y, z)

287 dimension of 912 x 900 x 60 grid points (Table 1, cf. Figure 2). As introduced in subsection

288 2.1.1above, the NCEP GDAS/FNL Global Gridded Analyses and Forecasts (0.25° x 0.25°,

289 every 6 h, 26 pressure levels)GFS was used as the IC/BCs of the model.

290
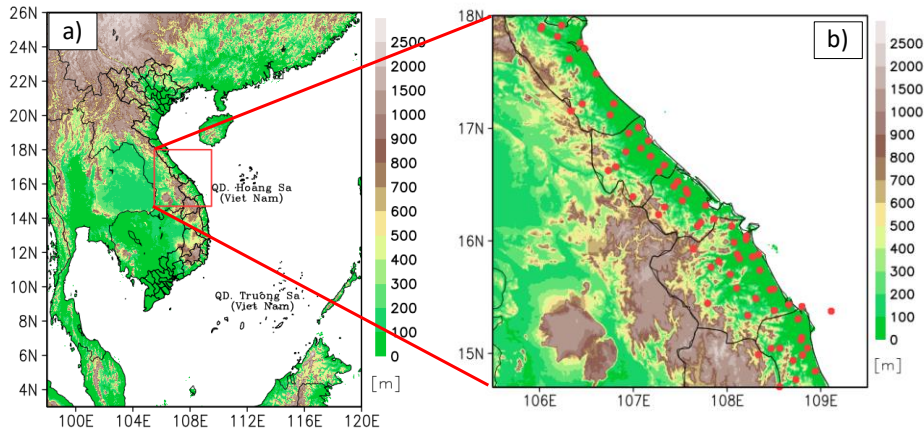
291 **Figure 2**. (a) The simulation domain of the CReSS model and topography (m, shaded)

292 used in the study. The red box marks the study area. (b) The distribution of the

293 observation stations (red dots) in the study area.

294

295 Table 1. The basic information of experiments.

Domain and Basic setup	
Model domain	3°–26°N; 98°–120°E
Grid dimension (x, y, z)	912 × 900 × 60
Grid spacing (x, y, z)	2.5 km × 2.5 km × 0.5 km*
Projection	Mercator
IC/BCs (including SST)	NCEP GDAS/FNL Global Gridded Analyses and Forecasts (0.25° × 0.25°, every 6 h, 26 pressure levels)

Topography (for CTRL only)	Digital elevation model by JMA at (1/120)° spatial resolution
Simulation length	192 h
Output frequency	1 hour
Model physical setup	
Cloud microphysics	Bulk cold-rain scheme (six species)
PBL parameterization	1.5-order closure with prediction of turbulent kinetic energy (Deardorff, 1980; Tsuboki and Sakakibara, 2007)
Surface processes	Energy and momentum fluxes, shortwave and longwave radiation (Kondo, 1976; Louis et al., 1982; Segami et al., 1989)
Soil model	41 levels, every 5 cm deep to 2 m

296 * The vertical grid spacing (Δz) of CReSS is stretched (smallest at bottom) and the

297 averaged value is given in the parentheses

298

299 2.3 Verification of model rainfall

300 In order to verify the model-simulated rainfall, some verification methods are used,

301 including (1) visual comparison between the model and the observation (from the 69

302 automated gauges over the study area), and (2) the objective verification using categorical

303 skill scores at various rainfall thresholds from the lowest at 0.05 mm up to 900 mm for

304 three-day total. These scores are presented below along with their formulas, perfect value,

305 and worst value, respectively. These scores are listed in Table 2 along with their formulas,

306 perfect value, and worst value, respectively. To apply these scores at a given threshold, the

model and observed value pairs at all verification points (gauge sites here, N) are first compared and classified to construct a 2×2 contingency table (Wilks, 2006). At any given site, if the event takes place (reaching the threshold) in both model and observation, the prediction is considered a hit (H). If the event occurs only in observation but not the model, it is a miss (M). If the event is predicted in the model but not observed, it is a false alarm (FA). Finally, if both model and observation show no event, the outcome is correct rejection (CR). After all the points are classified into the above four categories, the scores can be calculated by their corresponding formula as:

Bias Score (BS) = (H+FA)/(H+M), (1)

Probability of Detection (POD) = H/(H+M), (2)

False Alarms Ratio (FAR) = FA/(H+FA), (3)

Threat Score (TS) = H/(H+M+FA), (4)

The values of TS, POD, and FAR are all ranged from 0 to 1, and the higher value is the better for TS and POD, and conversely for FAR. For BS, its value can vary from 0 to N−1 and indicate the overestimation (underestimation) of the model for the events.

2.3.1 The Similarity Skill Score

In addition to the categorical scores, the Similarity Skill Score (SSS, Wang et al., 2022) is also applied to evaluate the model rainfall results, as

$$\text{SSS} = 1 - \frac{\frac{1}{N}\sum_{i=1}^{N}(F_i - O_i)^2}{\frac{1}{N}\sum_{i=1}^{N}F_i^2 + \frac{1}{N}\sum_{i=1}^{N}O_i^2} \qquad (5)$$

where N is the total number of verification points, F_i is the forecast rainfall amount, and O_i is the observed value, at the ith point among N, respectively. The SSS is a measure against the worst mean squared error (MSE) possible. The formula shows that a forecast with perfect skill has an SSS of 1, while a score of 0 means zero skill (model rainfall does not overlap with the observation anywhere).

332   2.3.2. The ensemble spread (standard deviation)

333   The ensemble spread is considered a measure of the difference between the members to

334   the ensemble mean and known as the standard deviation (SD). In other words, the ensemble

335   spread will reflect the diversity of all possible outcomes. Hence, the ensemble spread is

336   often applied to predict the magnitude of the forecast error. ~~If~~ For example, small spread

337   indicates high theoretical forecast accuracy, and large spread indicates low theoretical

338   forecast accuracy. Spread is computed by formulated below:

339

$$\text{SD} = \sqrt{\frac{\sum_{i=1}^{n}(x_i - \mu_x)^2}{n-1}}$$

340   (6)

341   where x_i is the prediction value of member i, μ_x is the ensemble mean, n is the number of

342   ensemble members.

343   2.3.3. Ensemble Sensitivity Analysis

344   As mentioned above, an ensemble forecast is a set of forecasts produced by many separate

345   forecasts with differences in initial conditions, respectively. Moreover, as we know, the

346   numerical weather forecasts are sensitive to small changes in initial conditions and

347   sensitivity analysis is considered a measure to improve forecasts through targeting

348   observations. Hence, this study used the ESA method which is introduced by Ancell and

349   Hakim (2007) to examine how a forecast variable responds to changes in initial conditions.

350   The ensemble sensitivity is computed by the formula:

351    $$\frac{\partial R}{\partial x_t} = \frac{COV(R, x_t)}{var(x_t)} \qquad (7)$$

352   Here, the response function R is chosen to be the areal-mean 24-h accumulated rainfall in

353   central Viet Nam (15.5°-16.3°N, 107.9°-108.6°E) on the rainiest day, from 12:00 UTC on

354   9 to 12:00 UTC on 10 December 2018. The starting time of this period, i.e., 12:00 UTC on

355   9 December, is defined as t_0. Various scalar variables are considered for x_t, while those

356 from 48 h earlier (t_{-48}, or 12:00 UTC on 7 December) to the time of t_0 at 24-h intervals.

357 The *COV* is the covariance of *R* and x_t, and *var* is the variance of x_t, respectively.

358 As the analysis in part 1, the D18 event is caused by combined effectively between the
359 atmospheric disturbances at lower levels, such as cold surge, easterly wind, and
360 topography, ensemble-based sensitivity analysis (ESA) has been applied for variables at
361 surface, near-surface, and mid-tropospheric levels to assess the sensitivity of initial
362 conditions to the predictability of the rainy field. In order to facilitate the comparison
363 among the impacts of different variables, this study normalized ESA results by using the
364 standardized anomaly in the denominator and expressed as the change in R (in mm) in
365 response to an increase in x_t by one SD.

3 Model results

367 3.1 Time-lagged 24-h QPFs by the CReSS model

368 In this section, time-lagged forecasts targeted for the 24-h period from 12:00 UTC on 9 to
369 12:00 UTC on 10 December in the D18 event by the 2.5-km CReSS model are presented
370 and evaluated. This study focuses on this 24-h period because this is the rainiest day with
371 24-h in-situ observed data exceeding 600 mm at some stations (Fig. 3 OBS). Figure 3
372 shows 25 possible scenarios of 24-h rainfall and average surface winds over the target
373 period produced by the lagged runs every 6 h, with the earliest initial time at 12:00 UTC
374 on 3 December and the latest one at 12:00 UTC on 9 December 2018, respectively. It is
375 immediately clear that several members made a rather good 24-h QPF not only in amounts,
376 but also in rainfall location and spatial distribution. These include most members
377 initialisedexecuted during 8-9 December, and also an impressive member that
378 initialisedstarted at 18:00 UTC on 4 December. In this latter member, a reasonably good
379 QPF was produced at a rather long lead time, almost five days prior to the beginning of the
380 target period (114 h). AA common feature among these good members is that they all
381 captured the direction and magnitude of surface winds quite well. On the other hand, most
382 other members did poorly in their QPFs, when initialisedexecuted before 06:00 UTC on 7

383 December at lead times beyond two days before the target period. In general, they also
384 could not predict the surface winds well enough.

385
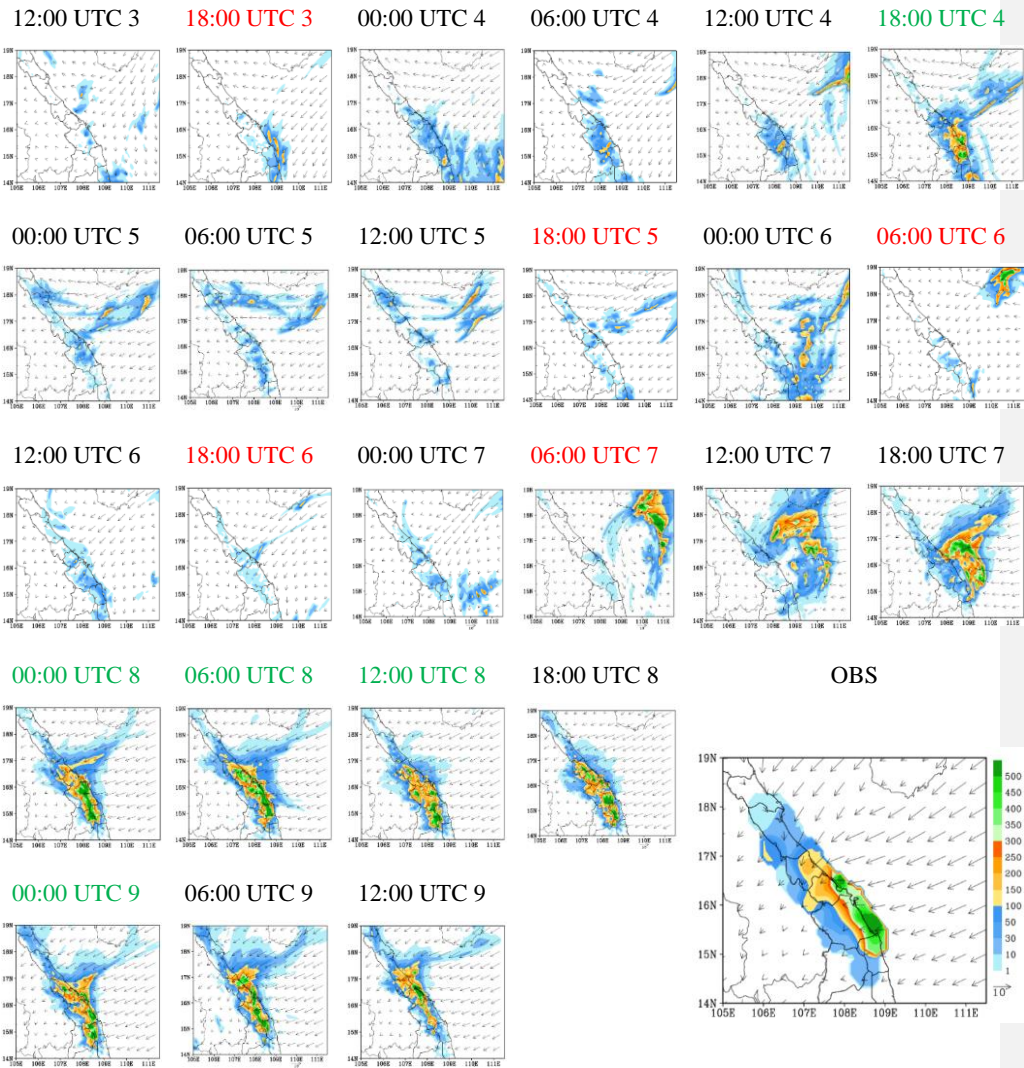
Figure 3. The predicted 24h accumulated rainfall (mm, shaded, scale on the right of panel OBS) and the mean surface horizontal wind (ms^{-1}, vector, reference length at panel OBS) on 10 December 2018 (from 12:00 UTC 9 December to 12:00 UTC 10 December 2018). The green color mark good members and the red color marks bad members. In OBS, 24h in-situ observed rainfall (mm, shaded) and the surface wind derived from ERA5 data (ms^{-1}, vector), adapted from Fig. 12f of Wang and Nguyen 2023.

The main reason for the significantly different forecast outcomes is elucidated in Fig. 4, which depicts the mean differences in five good members (those with initial times at 18:00 UTC on 4, 00:00, 06:00, and 12:00 UTC on 8, and 00:00 UTC on 9 December) from five bad ones (those ran at 18:00 UTC on 3, 18:00 UTC on 5, 06:00 and 18:00 UTC on 6, and 06:00 UTC on 7 December). In Fig. 4 (good minus bad members), it is clear that the surface easterly winds were much stronger and the relative humidity much higher surrounding central Viet Nam and its upstream areas in the GFS forecast data valid at 12:00 UTC on 9 December (used as BCs in CReSS runs) in the good members than in the bad ones. These

factors were identified as crucial for the extreme rainfall in the D18 event in Part 1, and thus the good CReSS members produced much more rainfall in central Viet Nam (Fig. 4b).

404 ~~Figure 4. The difference in (a) input data (boundary conditions) and (b) CReSS output~~
405 ~~between averaged 5 good members (members ran at 18:00 UTC 4, 00:00 UTC 8, 06:00~~
406 ~~UTC 8, 12:00 UTC 8, 00:00 UTC 9) and 5 bad members (members ran at 18:00 UTC 3,~~
407 ~~18:00 UTC 5, 06:00 UTC 6, 18:00 UTC 6, 06:00 UTC 7). For input data, relative humidity~~
408 ~~(%, shaded) and surface wind (ms^{-1}, vector) at 12:00 UTC December 9 2018. For CReSS~~
409 ~~output, 24-h accumulated rainfall (mm, shaded) and surface wind (ms^{-1}, vector).~~

410 Furthermore, ~~A~~as we know, ensemble weather forecasts are a set of forecasts from multiple
411 members that represent the range of future weather possibilities, and the simplest way to
412 use them is through the ensemble mean (that emphasizes the features that the members
413 agree upon). In order to see how good CReSS can predict the D18 event with the time-
414 lagged strategy, from possible scenarios of 24 hours of rainfall of 10th December that
415 produced by CReSS, This study has grouped scenarios and computed them into different
416 lead times using the range of their initial times. It can be clearly seen in Fig. 4~~5~~ that the
417 rainfall produced by Fifth 4 (12 UTC 7 - 06 UTC 8 Dec) and Sixth 4 (12 UTC 8 - 06 UTC
418 9 Dec) members is quite similar to observed data, not only rainfall amount but also the
419 locations of significant rainbands and regions that concentrate mainly rainfall. For other
420 subgroup scenarios, the model made the rainfall scenarios much lower than observed
421 rainfall data. In which, third 4 (12 UTC 5 - 06 UTC 6 Dec) and fourth 4 (12 UTC 6 - 06
422 UTC 7 Dec) members are the lowest. It can be relevant to the model that did not predict
423 well the wind fields in every single running at extend ranges (after day 3) as analyzed
424 previous. The rainfall of second 4 (12 UTC 4 - 06 UTC 5 Dec) members is the highest in
425 these subgroup scenarios due to a single good forecast initialised at 1800 UTC on 4 Dec
426 ~~the model having single good predict at 18:00 UTC on 4~~ [Fig. 3. (18:00 UTC 4)].

427

428

429

430

431

432

433

Lead time | First 4 members | Second 4 members | Third 4 members | Fourth 4 members

24h rainfall

Lead time | Fifth 4 members | Sixth 4 members | Last one member

24h rainfall

GPM   OBS

644.4
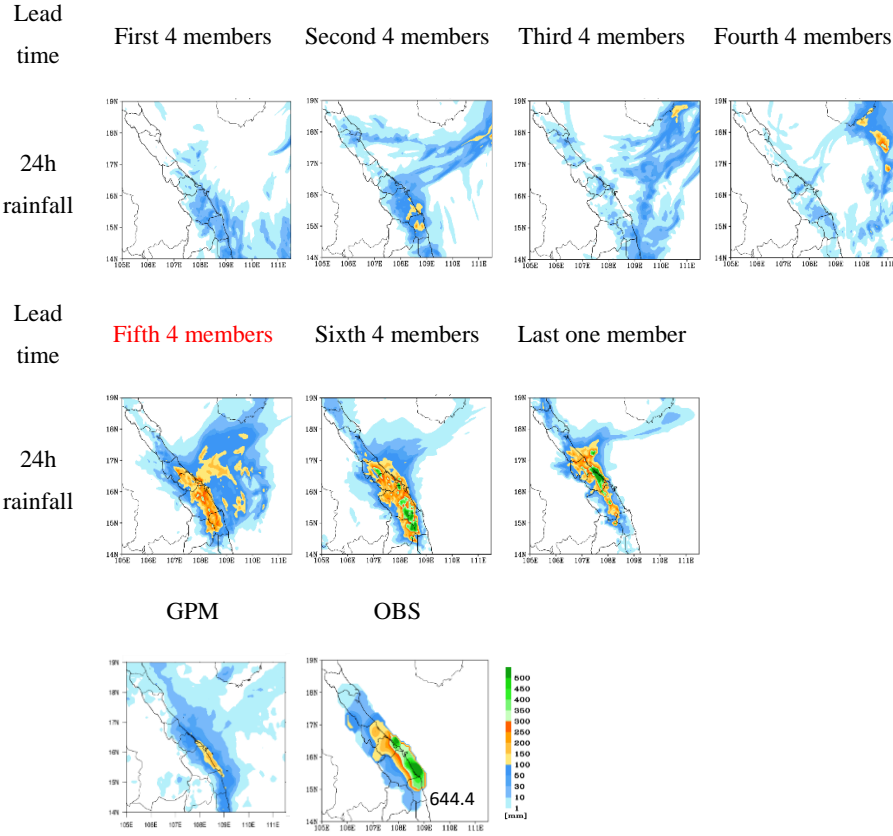
Figure 45. The predicted 24h rainfall by subgroup members, 24h accumulated rainfall by the Global Precipitation Measurement (GPM) estimate (IMERG Final Run product), 24h observed rainfall (mm, peak amount labeled at the lower-right corner) for the period of 12:00 UTC 9 December – 12:00 UTC 10 December 2018 as labelled. The same color bar (lower right) is used for all panels.

439

Besides the evaluation on time-lagged results using batches of fixed number of successive
runs (every 4 members) as presented above, this study also grouped the members using
different ensemble sizes based on their behavior in order to better assess the temporal
evolution of forecast uncertainty and event predictability as the lead time shortened.
Particularly, this study divided the 25 members into several subgroups as shown in Fig. 5̶6̶,
including the first eight members (those executed during 12:00 UTC 3 − 06:00 UTC 5
December), the middle eight members (run between 12:00 UTC 5 and 06:00 UTC 7
December), the last nine members (12:00 UTC 7−12:00 UTC 9 December), and the last
five members (12:00 UTC 8−12:00 UTC 9 December), respectively. In other words, the
last five members were those executed within 0-24 h (1 day) prior to the beginning of the
target period, and so on. In Fig. 5̶6̶, it is clear that both the ensemble means from the last
five and the last nine members compare quite favorable to the observation, not only in the
accumulated amount but also in spatial distribution of rainfall. This indicates that the model
could produce QPFs at fairly good quality and rather consistently since the time as early as
roughly 48 h prior to the commencement of the rainfall event (also Fig. 3). These two sub-
ensemble groups within the short range gave much better quality in QPFs than the other
sub-groups executed before them at longer lead times, including the first eight, middle
eight, and all 25 members. In terms of skill scores, for example, the mean QPF by the last
five members have TS = 0.4, POD = 0.8, FB = 1.5, and FAR = 0.5 at 100 mm (per 24 h),
while the last nine members give similar scores of TS = 0.5, POD = 0.8, FB = 1.4, and
FAR = 0.5 (Figs. 6̶7̶a-d), respectively. On the contrary, the mean QPFs from both the
middle eight and first eight members only yield zero scores in TS, POD, and FB with no
skill in FAR at 100 mm, obviously due to not enough rainfall in central Viet Nam in most
of their members. At 200 mm (per 24 h), similarly, the last five members (TS = 0.2, POD
= 0.4, FB = 1.4, and FAR = 0.7) and the last nine members (TS = 0.3, POD = 0.5, FB =
1.2, and FAR = 0.6) again produce much better scores in QPFs, compared to no skill in all
four scores in QPFs from the middle eight, first eight, and all 25 members (Fig. 7̶8̶a-d). In

467 SSS, the mean from the last nine members exhibits the highest score (0.64), the middle
468 eight members have the lowest score (0.04), and the mean from all 25 members is 0.43
469 (Fig. 6~~7~~e).

470
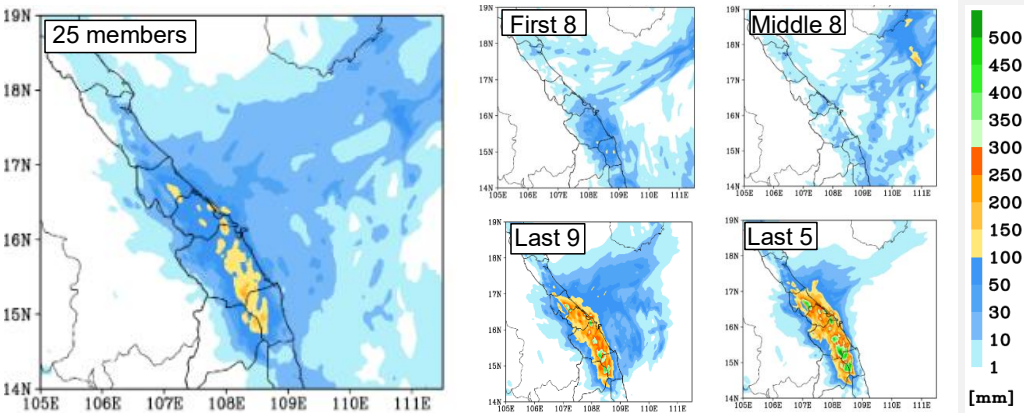
471

472 **Figure 5~~6~~**. Ensemble mean rainfall (shaded, scale on the right) from all 25 time-lagged
473 members, executed every 6 h from 12:00 UTC 3 December to 12:00 UTC 9 December, for
474 the 24h period from 12:00 UTC 9 December to 12:00 UTC 10 December.
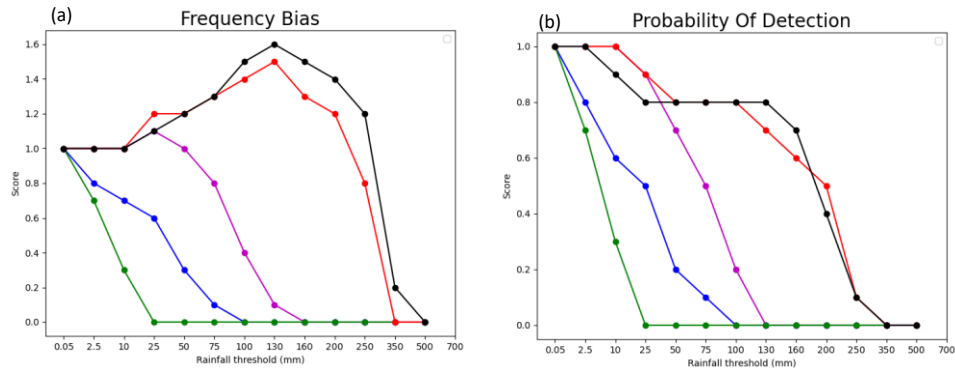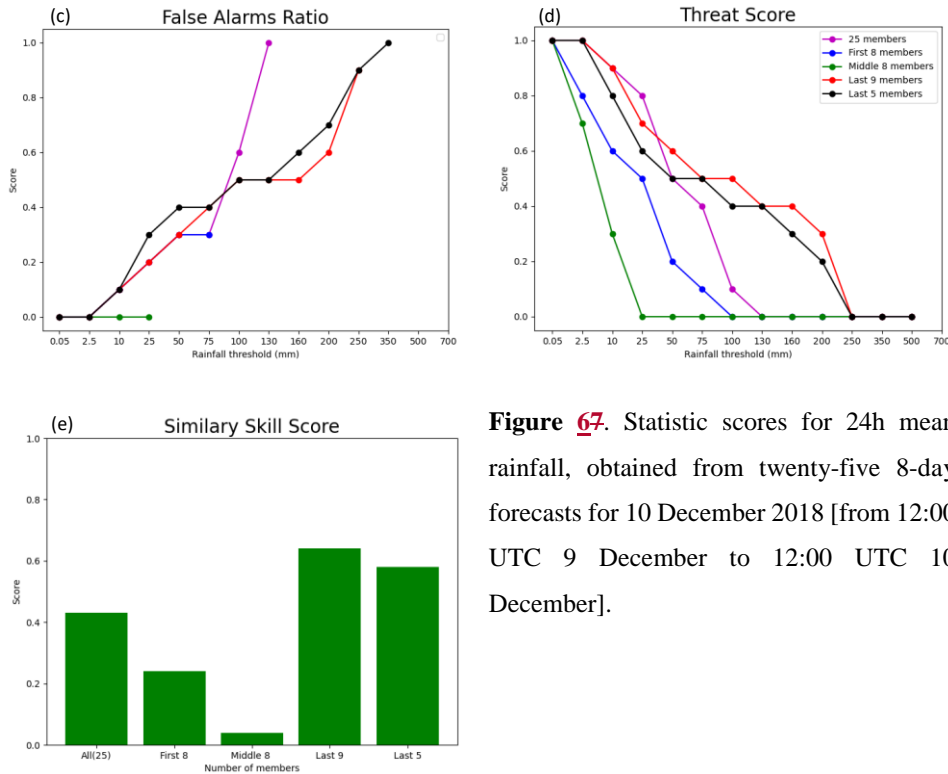
Figure 67. Statistic scores for 24h mean rainfall, obtained from twenty-five 8-day forecasts for 10 December 2018 [from 12:00 UTC 9 December to 12:00 UTC 10 December].

475

476   However, as indicated by the SD, the spreads in rainfall scenarios in both ensembles from

477   the last five and nine members are quite large (Fig. 78). Thus, while the lagged members

478   can produce a wide range of possible rainfall scenarios for the D18 event, which is the

479   main purpose of an ensemble as reviewed (Section 1), the members often cannot agree on

480   the precise locations of heavy rainfall. Given the small scale of local convection during the

481   event, this result is perhaps anticipated. On the other hand, the maxima in spread are >160

482   mm in Fig. 78 among the last nine members, and reasonable in magnitude compared to the

483   peak amounts of about 400 mm in the ensemble mean. In any case, Figs. 67 and 78 indicate

484   that the predictability of the D18 event changed considerably with time, and the 2.5-km

485 CReSS has a good skill in QPFs inside the short range (≤ 72 h). However, it is difficult to
486 predict the event successfully at longer lead times.

487

488

489
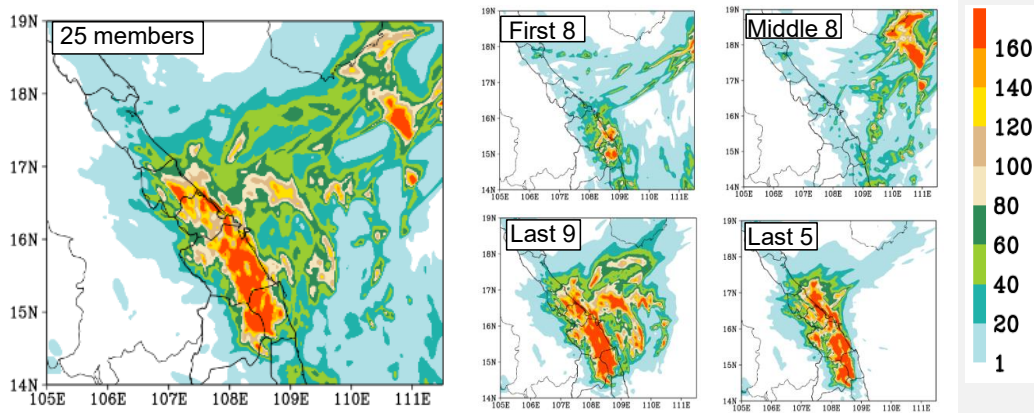
490 **Figure 78**. The spread (shaded, scale on the right) from all 25 time-lagged members,
491 executed every 6 h from 12:00 UTC 3 December to 12:00 UTC 9 December, for the 24h
492 period from 12:00 UTC 9 December to 12:00 UTC 10 December.

493

494 The probability information derived from the sub-ensemble groups at four different rainfall
495 thresholds from 100 to 450 mm is shown in Fig. 89, in which the increase in heavy-rainfall
496 probability in central Viet Nam and thus the predictability of the event with time is also
497 evident. From the first eight members executed at the longest range (≥ 102 h prior to rainfall
498 accumulation), there is only a 10-25% chance in parts of central Viet Nam to receive at
499 least 100 mm of rainfall (from 12:00 UTC 9 to 12:00 UTC 10 December). The probability
500 is even lower from the middle eight members (run between 54-96 h prior to target period),
501 as their SSS is the lowest among all sub-ensemble groups and only a couple of the runs

502 could reach 100 mm anywhere inland in central Viet Nam. As the lead time shortens to

503 inside the short range, the probabilities to have ≥ 100 mm of rainfall increase dramatically,

504 to roughly 70-80 % in the last nine members and further to over 80-90% in the last five

505 members. Due to the contribution from later members, about 20-40% of all 25 members

506 can reach 100 mm inland. Toward higher thresholds, the probabilities decrease in Fig. 8~~9~~

507 as expected, so are the areal sizes actually reaching those thresholds (red contours). At the

508 highest value of 450 mm, the ensembles in general show less than about 20% and 30%

509 chances for its occurrence from the last five and last nine members, respectively, and the

510 high probability areas are also slightly more inland than the observed one.

511
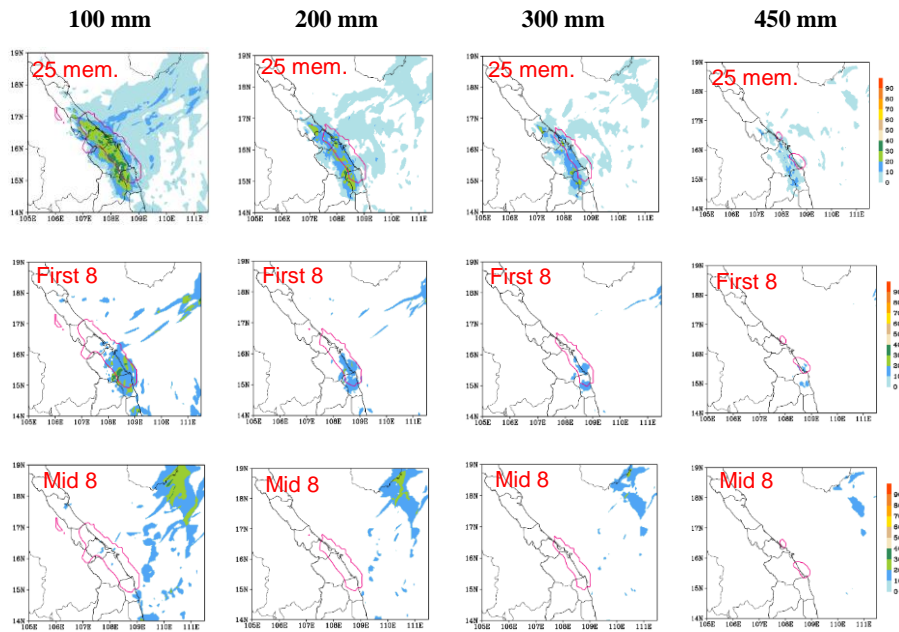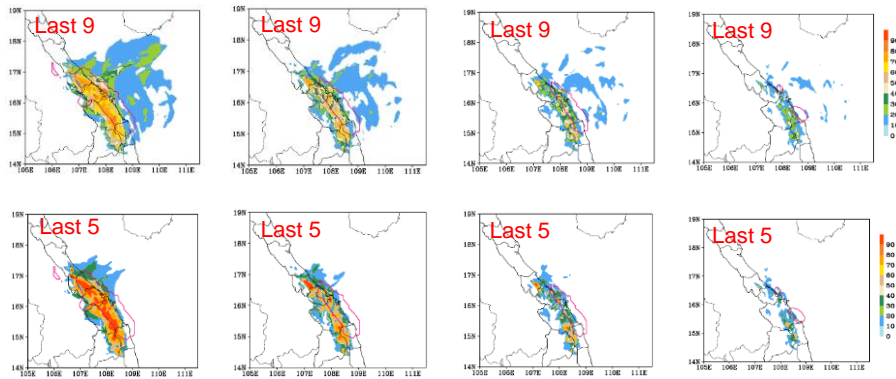
Figure 89. Probability distribution (%; shaded, scale on the right) from all 25 time-lagged members, executed every 6 h from 12:00 UTC 3 December to 12:00 UTC 9 December, reaching thresholds of 100, 200, 300, and 450 mm, for the 24h period from 12:00 UTC 9 December to 12:00 UTC 10 December. The observed areas at the same thresholds are depicted by the pink contours. For each picture, red labeled at the top-left corner show the number of members grouped to calculate the probability distribution.

3.2 Ensemble-based sensitivity analysis

The results in part 3.1 above reveal that the CReSS model with a horizontal resolution of 2.5 km had well QPF predicted the rainiest day of the event while other models can't capture it. Therefore, this part was made rely on this good performance.

Firstly, Figure 9 shown that Tthe main reason for the significantly different forecast outcomes is elucidated in Fig. 4, which depicts the mean differences in between five good members (those with initial times at 18:00 UTC on 4, 00:00, 06:00, and 12:00 UTC on 8, and 00:00 UTC on 9 December) fromand five bad ones (those ran at 18:00 UTC on 3, 18:00 UTC on 5, 06:00 and 18:00 UTC on 6, and 06:00 UTC on 7 December). In Fig. 4 (good minus bad members), it is clear that there are significant differences in the input datasets. Specifically, the surface easterly winds were much stronger and the relative

530 humidity much higher surrounding central Viet Nam and its upstream areas in the GFS
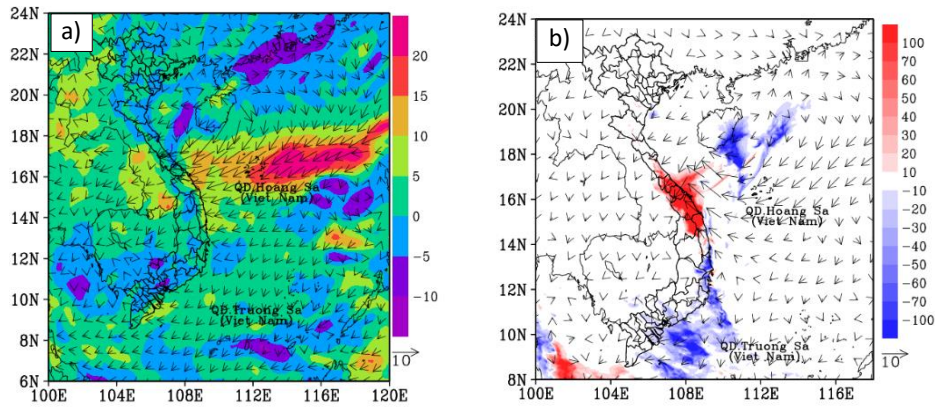
531 forecast data valid at 12:00 UTC on 9 December (used as BCs in CReSS runs) in the good

532 members than in the bad ones (Fig. 9a). These factors were identified as crucial for the

533 extreme rainfall in the D18 event in Part 1, and thus the good CReSS members produced

534 much more rainfall in central Viet Nam (Fig. 94b).

535
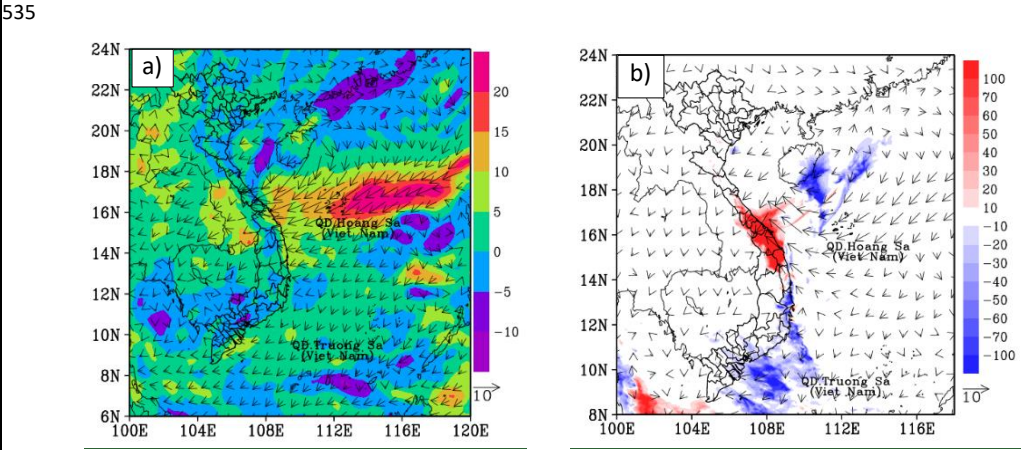
536

537 **Figure 9**4. The difference in (a) input data (boundary conditions) and (b) CReSS output

538 between averaged 5 good members (members ran at 18:00 UTC 4, 00:00 UTC 8, 06:00

UTC 8, 12:00 UTC 8, 00:00 UTC 9) and 5 bad members (members ran at 18:00 UTC 3, 18:00 UTC 5, 06:00 UTC 6, 18:00 UTC 6, 06:00 UTC 7). For input data, relative humidity (%, shaded) and surface wind (ms^{-1}, vector) at 12:00 UTC December 9 2018. For CReSS output, 24-h accumulated rainfall (mm, shaded) and surface wind (ms^{-1}, vector).

Meanwhile, Figure 10 show the difference in the evolution of synoptic-scale patterns (features), with a zoom in the study area. To be more specific, Figures 10a show the difference (model output - NCEP FNL analysis data) in the horizontal wind and vertical velocity between averaged 5 good members and the NCEP FNL analysis data at 925 hPa and at 12 UTC 09 is small although each member was initialized at different lead time. It implies that these members captured well the evolution of weather patterns of this event. Additionally, the model vertical velocity is observed greater than NCEP FNL analysis data. Therefore, these members produced the rainfall closer to observed rainfall even the study area is a complex terrain. Contrarily, bad members poorly captured the evolution of weather patterns (Fig. 10b). Consequently, these members can't produce rainfall close to the observed rainfall data.

Furthermore, Figs. 10d indicates the difference in initial data of the member that initialized at 18:00 UTC 04 is very small, especially over the study area. The evolution of weather patterns every 24-hours based on this initial data is also observed small at first 3 days lead time. The difference then developed larger. However, the difference is smaller at 12:00 UTC 09 (approximate 5 days lead time) (Figs. 10e,f,g). Compare to this, the bad member initialized at 18:00 UTC 06 (2-days lead time shorter) have a larger difference in the initialized state of atmosphere, even this difference is also small in comparison with NCEP FNL analysis data (Fig. 10h). this difference then led to a larger difference in evolution of weather patterns, as observed at Figs. 10 i, j, and k.
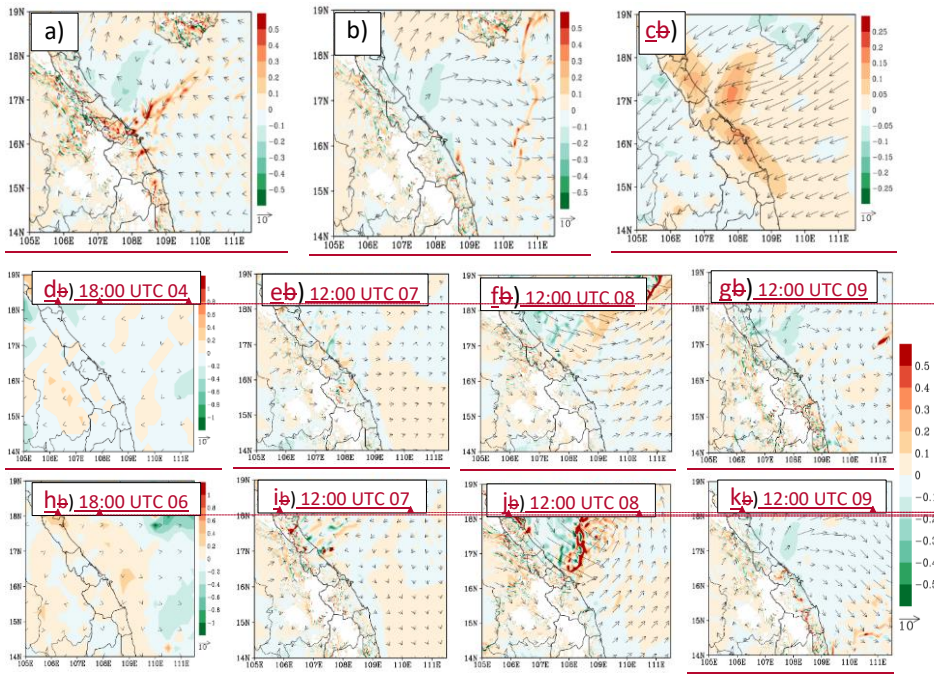
565

Figure 10. The difference in the horizontal wind (ms^{-1}, vector, reference length at the low-right corner of the panel), and vertical velocity (ms^{-1}, shaded, the reference color scale is on the right of panel) between (a) averaged 5 good members and (b) averaged 5 bad members and the NCEP FNL analysis data at 925 hPa and at 12 UTC 09. (c) The NCEP FNL analysis horizontal wind (ms^{-1}, vector, reference length at the low-right corner of the panel) and vertical velocity (ms^{-1}, shaded) at 925 mb and at 12 UTC 09. (d) The difference in the horizontal wind (ms^{-1}, vector, reference length at the low-right corner of the panel), and relative humidity (%, shaded, the reference color scale is on the right of panel) between the initial data of a good member at a longer lead time (at 1800 UTC 4 Dec) and the NCEP FNL analysis data at 925 hPa. (e), (f), and (g) present the difference in the evolution of weather features with time by this good member. (h) as in (d) but for a bad member (member was ran at 1800 UTC 6 Dec). (i), (j) and (k) as in (e), (f), and (g), respectively, but for mentioned bad member.

579

580 , (i), (j), and (k) by a bad member (member ran at 18 UTC 05). Compared variables are

581 horizontal wind at 925 hPa (ms^{-1}, vector, reference length at the low-right corner of the

582 panel) and vertical velocity (ms^{-1}, shaded, the reference color scale is on the right of panel)

583 The NCEP FNL analysis horizontal wind (ms^{-1}, vector, reference length at the low-right

584 corner of the panel) and vertical velocity (ms^{-1}, shaded) at 925 mb and at 12 UTC 09.

585 These not only indicate that it is still possible to have good forecasts at a lead time of up to

586 5 days but also show the good performance of CReSS in predictability of the event at longer

587 lead time.

588 Additionally, these also reaffirm that a very small difference in the initialized data could

589 then lead to a very different in the outcome, especially as the forecast range increases. On

590 the other hand, the predicted rainfall is very sensitive with every small difference in the

591 initial data. Besides, as pointed out Part 1 that the low-level wind convergence led to

592 moisture convergence and these conditions resulted in the D18 event. And the southward

593 movement of the low-level wind convergence also dictated the movement of heavy

594 rainband during the event. Therefore, ESA was applied on relevant variables, including the

595 zonal and meridional components of wind, and water mixing ratio. The quantitative results

596 are shown in Figs. 11-13.

597 To be more specific, Figure 11 shows the sensitivity of mean 24-h total rainfall inside the

598 green box in central Viet Nam (R) to zonal (u) and meridional (v) wind components and

599 water vapor mixing ratio (q_v) at the altitude of 100 meters surface, and the ensemble mean

600 are also plotted. It is clear that the sensitivity of rainfall to these variables is lower at longer

601 forecast ranges and becomes higher at shorter lead times. Specifically, from two days

602 before (t_{-48}) to the starting time of the accumulation period (t_0), the sensitivity of rainfall

603 to u-wind over the SCS and along the coast of central Viet Nam turned more negative,

604 indicating heavier rainfall associated with stronger easterly winds ($u < 0$) near the surface,

605 especially in areas immediately upstream at t_0 (Figs. 11a-d). The rainfall's sensitivity to v-

606 wind leading to t_0, on the other hand, exhibited a dipole structure, with negative values to

607 the north-northwest and positive values to the south-southeast across central Viet Nam and

608 the upstream ocean. This structure indicates a stronger confluence in northeasterly winds

609 over the region in rainier members, consistent with the results in Part 1. In Figs. 1~~01~~de-~~f~~h,

610 the increase in v-wind just south of central Viet Nam is particularly evident, from −10 mm

611 (per SD, SD =2 ms^{-1}) at t_{-48} to over +70 mm (per SD – Standard deviation, SD=2-4 ms^{-1})

612 at t_0. Thus, the precipitation amount in the D18 event in central Viet Nam is highly sensitive

613 to the northeasterly winds in short range forecasts. ~~In contrast~~Similarly, ~~compared to the~~

614 ~~winds,~~ the rainfall was ~~less~~ also highly-sensitive to the water vapor amount as shown in

615 Figs. 1~~10~~gi-~~i~~l.
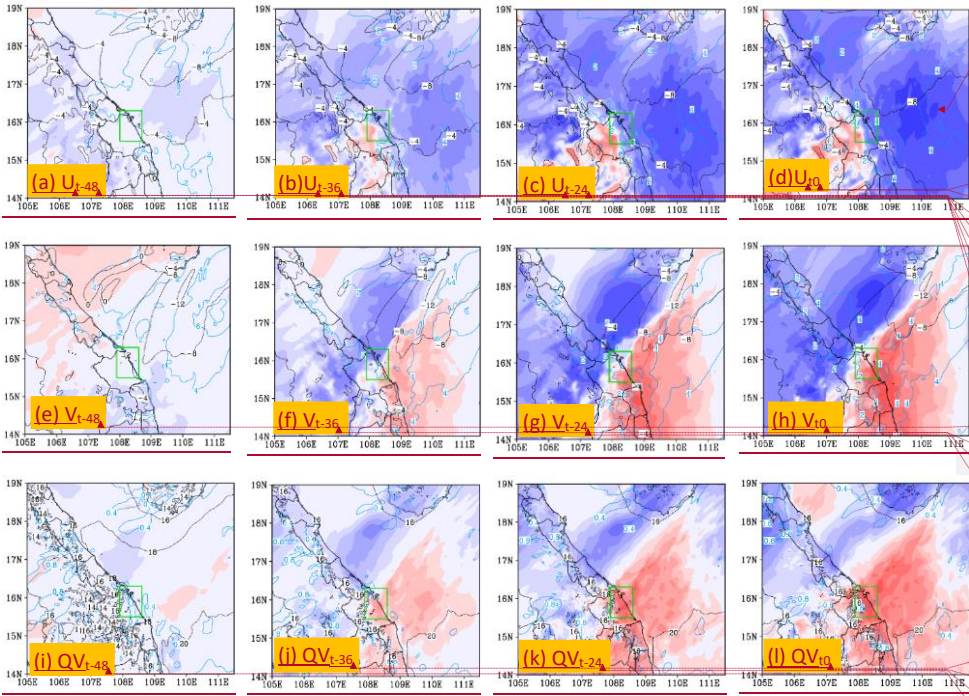
618

619

620

621

622

623

624

625

626

627

628

629

Figure 110. The sensitivity (mm, per SD, color, scale on the right) of areal-mean 24h accumulated rainfall in central Viet Nam starting from t_0 (i.e., R, averaging area depicted in green box) to surface wind components (ms^{-1}, shaded) and the ensemble mean (contours, every 4 ms^{-1}) and to surface water vapor mixing ratio (r, g kg^{-1}) and its ensemble mean (contours, every 0.06 g kg^{-1}) at different times at 24h intervals from (a) t_{-48} to (f) t_0. The time of t_0 is 12:00 UTC 9 December 2018. In which, (a), (b), (c), (d) for the zonal wind component. (d), (e), (f), (g), (h) for the meridional wind component, and (g), (h), (i), (j), (k), (l) for surface water vapor mixing ratio. The standard deviation is exhibited by the medium blue contours.

Slightly higher at 1476 m (near 850 hPa), where easterly flow prevailed during the D18 event (see Fig. 3b in Part 1), the sensitivity of rainfall to winds exhibits similar spatial patterns (Figs. 121a-hf) to those at the altitude of 100 meters surface (Figs. 11a-h), with

stronger easterly winds and larger confluence in association with heavier rainfall. ~~On the~~ ~~other hand~~Similarly, ~~note that~~ the rainfall ~~becomes~~ still shows ~~more~~ high sensitive to mixing ratio in central Viet Nam at this level (Figs. 12~~11gi-i~~l), especially at shorter lead times,~~ compared to its insensitivity to surface moisture amount~~. Presumably, this positive correlation is due to upward transport of moisture, as the ascending motion in convective clouds could become larger at this level.

653

654

655

656

657

658

659
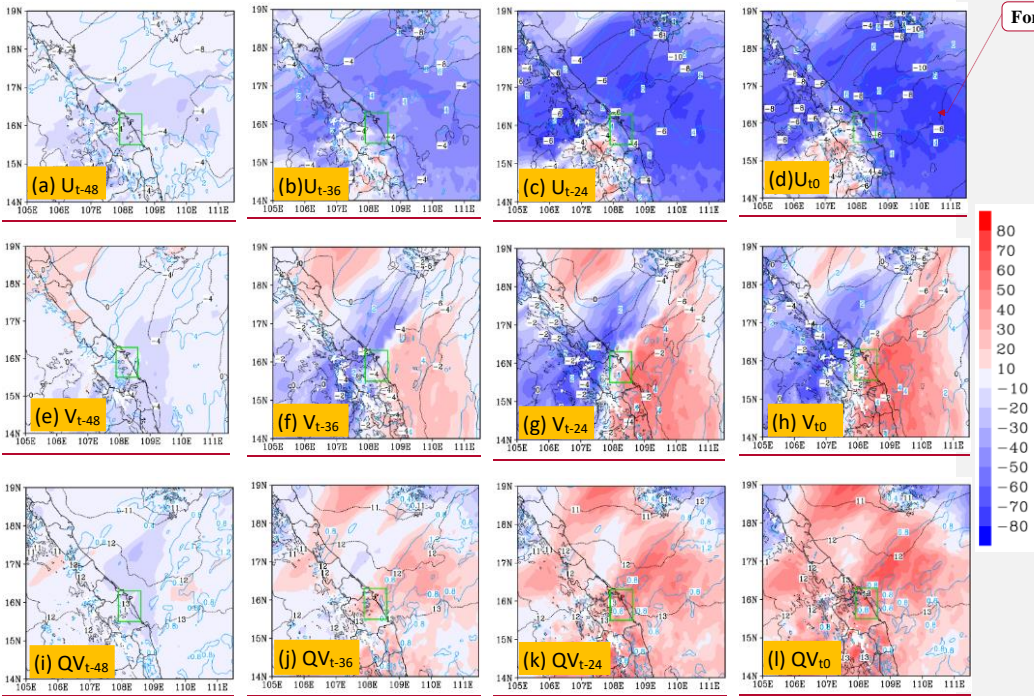
Figure 1~~1~~2. The sensitivity (mm, per SD, color, scale on the right) of 24h accumulated rainfall in central Viet Nam starting from t_0 (i.e., R, averaging area depicted in green box) to the wind components (ms^{-1}, shaded) and the ensemble mean (contours, every ~~4~~ 2 ms^{-1}) and to water vapor mixing ratio (r, g kg^{-1}) and its ensemble mean (contours, every 0.~~06~~ 4 g kg^{-1}) at attitude of 1476 m and at different times at 24h intervals from (a) t_{-48} to (f) t_0. The time of t_0 is 12:00 UTC 9 December 2018. In which, (a), (b), (c), (d) for the zonal wind component. ~~(d),~~ (e), (f), (g), (h) for the meridional wind component, and ~~(g), (h),~~ (i), (j), (k), (l) for water vapor mixing ratio. The standard deviation is exhibited by the medium blue contours.   ¬¬

At the upper level of 5424 m (near 500 hPa), it is seen that from t_{-48} to t_0, dipole structures developed in the sensitivity patterns to both u and v winds (Figs. 1~~3~~2a-~~h~~f). To u winds, positive sensitivity up to about +70 mm (per SD, SD=2-4 ms^{-1} depends on t_x) existed to the south and negative sensitivity up to −70 mm (per SD, SD=2-4 ms^{-1} depends on t_x) to the north of central Viet Nam. Meanwhile, positive sensitivity to v-wind appeared to the north and east with negative sensitivity to the south and west of the rainfall area. While the prevailing winds at 500 hPa were southeasterly over southern Viet Nam and southwesterly over northern Viet Nam during D18 (thus with anticyclonic curvature, see Fig. 3c in Part 1), the above sensitivity patterns, apparent at t_{-24} already, corresponded to stronger diffluence/divergence and a weaker anticyclone aloft to favor more rainfall. To q_v, positive

sensitivity signals up to +70 mm (per SD, SD=1.2 g kg⁻¹) also appeared over the rainfall

area at t_{-24} and t_0 (Figs. 12h13,i-l), and the reason is similar to those near 850 hPa in Fig.

11.
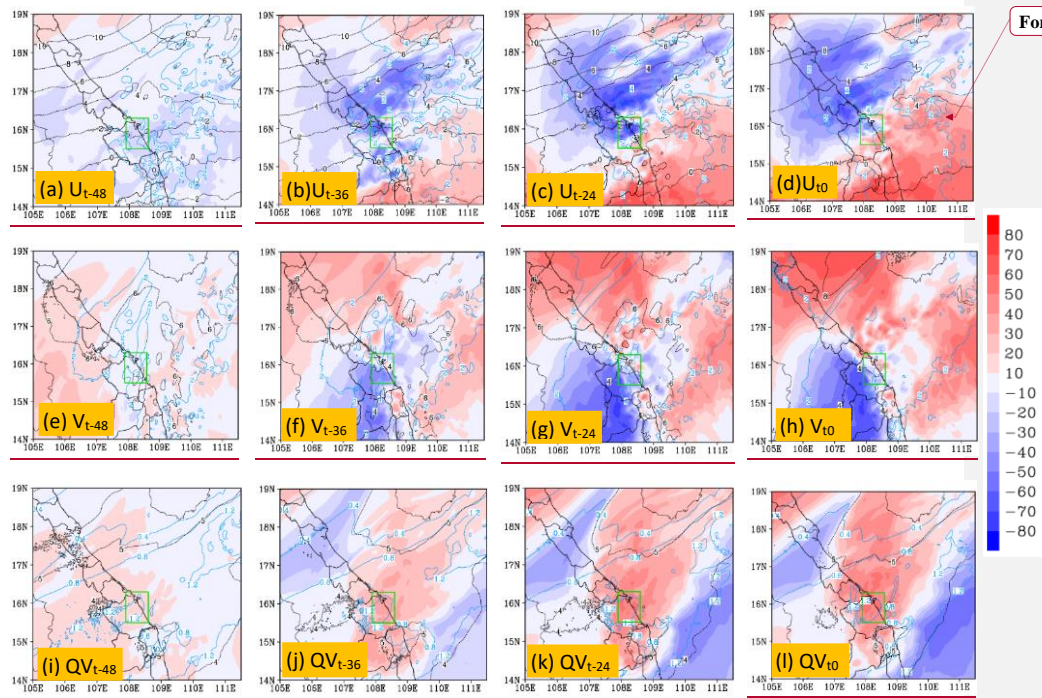
Formatted Table

689

690

691

692

693

694

695

Figure 1~~3~~2. The sensitivity (mm, per SD, color, scale on the right) of 24h accumulated rainfall in central Viet Nam starting from t_0 (i.e., R, averaging area depicted in green box) to the wind components (ms^{-1}, shaded) and the ensemble mean (contours, every ~~4~~ 2 ms^{-1}) and to water vapor mixing ratio (r, g kg^{-1}) and its ensemble mean (contours, every 0.~~06~~4 g kg^{-1}) at attitude of ~~54~~24 m and at different times at 24h intervals from (a) t_{-48} to (f) t_0. The time of t_0 is 12:00 UTC 9 December 2018. In which, (a), (b), (c), (d) for the zonal wind component. ~~(d),~~ (e), (f), (g), (h) for the meridional wind component, and ~~(g), (h),~~ (i), (j), (k), (l) for water vapor mixing ratio. The standard deviation is exhibited by the medium blue contours.   ¬¬

These ensemble-based sensitivity analyses indicated clearly that the synoptic pattern that caused the D18 event already developed at times more than 24h earlier

4 Conclusion

As high resolution is required in numerical models to predict heavy rainfall more successfully, the present work utilizes a time-lagged high-resolution ensemble forecast system and evaluates how well the D18 event (during 9-12 December 2018) in central Viet Nam can be predicted in advance before its occurrence. Using the CReSS model with a grid size of 2.5 km (912 × 900 in dimension with 60 vertical levels), ensemble forecasts were produced with a total of 29 time-lagged runs at 6-h intervals, each out to a forecast

range of 192 h (eight days). Our evaluation results in predictability indicate that the 2.5-km system predicted the rainfall fields on 10 December during the event fairly well, including both the amount and spatial distribution, within the short range at lead times of day 1, 2, and 3. More specifically, the SSS of QPFs at these three ranges are about 0.4, 0.6, and 0.7, respectively, with fairly consistent results among successive runs that indicate a reasonable predictability, despite some spread and disagreement on the precise locations of heavy rainfall. The above good results are due to the model's capability to better predict the conditions in the lower troposphere such as the wind fields.

At lead times longer than three days, however, the predictability of the event is lowered due to a higher level of forecast uncertainty, and the quality of QPFs drops with significant under-prediction. Nevertheless, good QPFs are still possible occasionally. At lead time beyond six days, it is challenging to achieve a good QPF at thresholds greater than 100 mm even with a high-resolution model. This is presumably linked to the rapid evolution of atmospheric conditions surrounding Viet Nam in a tropical environment. In the present study, a CRM is applied to forecast extreme rainfall in central Viet Nam for the first time. Although still with certain limitations, our results do indicate hope to predict such events successfully beforehand, at least within the short range. Therefore, based on the present work, more studies on the predictability of extreme rainfall in Viet Nam are recommended in the near future.

The present study also performed an ensemble sensitivity analysis to identify the important factors that influenced the 24-h rainfall amount in central Viet Nam in the D18 event. The result shows that the rainfall is most sensitive to the wind conditions in the lower troposphere leading to the event, with more rain associated with stronger northeasterly to easterly winds and their confluence. In additionSimilarly, the rainfall also shows some strong sensitivity to the moisture amount, not only at the surface but alsoand winds further aloft at the upper levels. Besides, ESA also indicated that the synoptic pattern that caused the D18 event already developed at timing earlier in the past. Furthermore, Iin the ESA, the finer-scale features (convection) are also seen to link to synoptic conditions in their

background, implying that it is meaningful to apply ESA to control the perturbations in initial fields.

Acknowledgements: This study was supported by the project "*Research on the application of the Cloud-resolving model integrated with the regional numerical model to a 6-hour accumulated quantitative precipitation forecast with 24-48 hours lead time for Mid-Central Viet Nam*", which is funded by the Ministry of Natural Resources and Environment (MONRE) under grant no. TNMT.2023.06.07, and also by the National Science and Technology Council (NSTC) of Taiwan under grants MOST 111-2111-M-003-005 and MOST 111-2625-M-003-001.

Code and data availability. The CReSS model used in this study and its user's guide are available at the model website at http://www.rain.hyarc.nagoya-u.ac.jp/~tsuboki/cress_html/src_cress/CReSS2223_users_guide_eng.pdf (last access: 6 July 2023; Tsuboki and Sakakibara, 2007). The TIGGE data and its information are available at https://confluence.ecmwf.int/display/TIGGE/TIGGE+archive. The NCEP GFS dataset and its description are available at https://rda.ucar.edu/datasets/ds084.1/. The NCEP FNL operational global gridded analysis data and its information is available at https://rda.ucar.edu/datasets/d083003/#.

Author contributions. **Duc Van Nguyen** prepared datasets, executed the model experiments, performed the analysis, and prepared the first draft of the manuscript. **Chung-Chieh Wang** also prepared the first draft and provided the funding, guidance and suggestions during the study, and they participated in the revision of the manuscript. **Kien Ba Truong** provided the funding and participated revising of the manuscript. **Thang Van Vu**, **Pham Thi Thanh Nga**, and **Pi-Yu Chuang** also participated in the revision of the manuscript.

Competing interests. The authors declare that they have no conflict of interest.

References

Ancell, and Hakim, G. J.: Comparing adjoint- and ensemble sensitivity analysis with applications to observation targeting. Mon. Wea. Rev., 135, 4117–4134, doi:10.1175/2007MWR1904.1, 2007.

Cotton, W. R., Tripoli, G. J., Rauber, R. M., and Mulvihill, E. A.: Numerical simulation of the effects of varying ice crystal nucleation rates and aggregation processes on orographic snowfall. J. Appl. Meteorol. Clim., 25, 1658–1680, 1986.

Coleman,A. A., and Ancell, B. C.:Toward the improvement of high-impact probabilistic forecasts with a sensitivity-based convective-scale ensemble subsetting technique. Mon. Wea. Rev., 148, 4995–5014, https://doi.org/10.1175/MWRD-20-0043.1, 2020.

Deardorff, J. W.: Stratocumulus-capped mixed layers derived from a three-dimensional model. Bound.-Lay. Meteorol., 18, 495–527, 1980.

Hu, C.-C., and Wu, C.-C.: Ensemble sensitivity analysis of tropical cyclone intensification rate during the development stage. J. Atmos. Sci., 77, 3387–3405, https://doi.org/10.1175/JAS-D-19-0196.1, 2020.

Hoa, V. V.: Comparative study skills rain forecast the middle part and central highland of several global models (In Viet Namese). Viet Nam journal of Hydrometeorology. V. 667 No. 07 (2016), 2016.

Hohenegger, C., and Schär, C.: Predictability and error growth dynamics in cloud-resolving models. J. Atmos. Sci., 64, 4467–4478, https://doi.org/10.1175/2007JAS2143.1, 2007.

Ikawa, M. and Saito, K.: Description of a non-hydrostatic model developed at the Forecast Research Department of the MRI, MRI Technical report 28, Japan Meteorological Agency, Tsukuba, Japan, ISSN: 0386-4049, 1991.

792 Kerr, C. A., Stensrud, D. J. and Wang, X.: Diagnosing convective dependencies on near-
793   storm environments using ensemble sensitivity analyses. Mon. Wea. Rev., 147, 495–
794   517, https://doi.org/10.1175/MWRD-18-0140.1, 2019.

795 Kondo, J.: Heat balance of the China Sea during the air mass transformation experiment.
796   J. Meteorol. Soc. Jpn., 54, 382–398, https://doi.org/10.2151/jmsj1965.54.6_382, 1976.

797 Leith, C. E.: Theoretical skill of Monte Carlo forecasts. Mon. Wea. Rev., 102, 409–
798   418, 1974.

799 Lin, Y.-L., Farley, R. D., and Orville, H. D.: Bulk parameterization of the snow field in a
800   cloud model. J. Appl. Meteorol. Clim., 22, 1065–1092, 1983.

801 Louis, J. F., Tiedtke, M., and Geleyn, J. F.: A short history of the operational PBL
802   parameterization at ECMWF, in: Proceedings of Workshop on Planetary Boundary
803   Layer Parameterization, 25– 27 November 1981, Shinfield Park, Reading, UK, 59–79,
804   1982.

805 Lorenz, E.N.: The predictability of a flow which possesses many scales of motion. Tellus,
806   21, 289–307. https://doi.org/10.3402/tellusa.v21i3.10086, 1969.

807 Murphy, J. M.: The impact of ensemble forecasts on predictability. Quart. J. Roy.
808   Meteor. Soc., 114, 463–493, 1988.

809 Murakami, M.: Numerical modeling of dynamical and microphysical evolution of an
810   isolated convective cloud – the 19 July 1981 CCOPE cloud. J. Meteorol. Soc. Jpn., 68,
811   107–128, 1990.

812 Murakami, M., Clark, T. L., and Hall, W. D.: Numerical simulations of convective snow
813   clouds over the Sea of Japan: Two dimensional simulation of mixed layer development
814   and convective snow cloud formation. J. Meteorol. Soc. Jpn. 72, 43–62, 1994.

815 Nhu, D. H., Anh, N. X., Phong, N. B., Quang, N. D., and Hiep, V. N.: The role of
816   orographic effects on occurrence of the heavy rainfall event over central Viet Nam in

November 1999. Journal of Marine Science and Technology. V. 17, No. 4B(2017), 31-36, 2017.

Segami, A., Kurihara, K., Nakamura, H., Ueno, M., Takano, I., and Tatsumi, Y.: Operational mesoscale weather prediction with Japan Spectral Model. J. Meteorol. Soc. Jpn., 67, 907–924, https://doi.org/10.2151/jmsj1965.67.5_907, 1989.

Surcel, M., Zawadzki, I., and Yau, M. K.: On the filtering properties of ensemble averaging for storm-scale precipitation forecasts. Mon. Wea. Rev., 142, 1093–1105, doi:10.1175/ MWR-D-13-00134.1, 2014.

Son, B. M. and Tan, P. V.: Experiments of heavy rainfall prediction over South of Central Viet Nam using MM5 (In VietNamese). Viet Nam Journal of Hydrometeorology., 4(580), 9−18, 2009.

Toan, T. N., Thanh, C., Phuong, P. T., and Anh, T. V.: Assessing the predictability of WRF model for heavy rain by cold air associated with the easterly wind at high-level patterns over mid-central Viet Nam (In VietNamese). VNU Journal of Science: Earth and Environmental Sciences. v. 34, n. 1S, dec. 2018. ISSN 2588-1094. https://js.vnu.edu.vn/EES/article/view/4328, 2018.

Torn, R.D., Hakim, G.J.: Initial condition sensitivity of western Pacific extratropical transitions determined using ensemble-based sensitivity analysis. Mon. Weather Rev. 137, 3388–3406. https://doi.org/10.1175/2009MWR2879.1, 2009.

Tsuboki, K. and Sakakibara, A.: Numerical Prediction of HighImpact Weather Systems: The Textbook for the Seventeenth IHP Training Course in 2007, Hydrospheric Atmospheric Research Center, Nagoya University, Nagoya, Japan, and UNESCO, Paris, France, 273 pp., http://www.rain.hyarc.nagoya-u.ac.jp/~tsuboki/ cress_html/src_cress/CReSS2223_users_guide_eng.pdf (last access: 1 May 2019), 2007.

Tuoi Tre news: https://tuoitre.vn/mien-trung-tiep-tuc-mua-lon-14-nguoi-chet-va-mat-tich-20181212201907413.htm (last ac-cess: 5 June 2024), 2018

Wang, C.-C.*, Kuo, H.-C., Yeh, T.-C., Chung, C.-H., Chen, Y.-H., Huang, S.-Y., Wang, Y.-W., and Liu, C.-H.: High-resolution quantitative precipitation forecasts and simulations by the Cloud-Resolving Storm Simulator (CReSS) for Typhoon Morakot (2009). J.Hydrol., 506, 26-41, http://dx.doi.org/10.1016/j.jhydrol.2013.02.018, 2013.

Wang. C.-C.*, Lin, B.-X., Chen, C.-T., and Lo, S.-H.: Quantifying the effects of long-term climate change on tropical cyclone rainfall using cloud-resolving models: Examples of two landfall typhoons in Taiwan. J. Climate, 2015.

Wang, C.-C.: On the calculation and correction of equitable threat score for model quantitative precipitation forecasts for small verification areas: The example of Taiwan. Wea. Forecasting, 29, 788–798, doi:10.1175/WAF-D-13-00087.1, 2014.

Wang, C.-C., Huang, S.-Y., Chen, S.-H., Chang, C.-S., and Tsuboki, K.: Cloud resolving typhoon rainfall ensemble forecasts for Taiwan with large domain and extended range through time-lagged approach. Wea. Forecasting, 31,151–172, doi:10.1175/WAF-D-15-0045.1, 2016.

Wang, C.-C., Li, M.-S., Chang, C.-S., Chuang, P.-Y., Chen, S.-H., and Tsuboki, K.: Ensemble-based sensitivity analysis and predictability of an extreme rainfall event over northern Taiwan in the Mei-yu season: The 2 June 2017 case. Atmos. Res., 259, 105684, https://doi.org/10.1016/j.atmosres.2021.105684, 2021.

Wang, C.-C., Tsai, C.-H., Jou, B. J.-D., and David, S. J.: Time-Lagged Ensemble Quantitative Precipitation Forecasts for Three Landfalling Typhoons in the Philippines Using the CReSS Model, Part I: Description and Verification against Rain-Gauge Observations. Atmosphere, 13, 1193, https://doi.org/10.3390/atmos13081193, 2022.

Wang, C.-C., and Nguyen, D. V.: Investigation of an extreme rainfall event during 8–12 December 2018 over central Viet Nam – Part 1: Analysis and cloud-resolving

868   simulation. Nat. Hazards Earth Syst. Sci., 23, 771–788, https://doi.org/10.5194/nhess-
869   23-771-2023, 2023.

870 Wang, C.-C., Chen, S.-H., Chen, Y.-H., Kuo, H.-C., Ruppert, Jr., J. H., and Tsuboki, K.:
871   Cloud-resolving time-lagged rainfall ensemble forecasts for typhoons in Taiwan:
872   Examples of Saola (2012), Soulik (2013), and Soudelor (2015). Wea. Clim. Extremes,
873   40, 100555, https://doi.org/10.1016/j.wace.2023.100555, 2023.

874 Wilks, D. S.: Statistical Methods in the Atmospheric Sciences. Academic Press, 648 pp.,
875   ISBN 13: 978-0-12-751966-1, 10: 0-12- 751966-1, 2006.

876